Reactivity of Xenon with Ice at Planetary Conditions

Chrystèle Sanloup*
UPMC Univ Paris 06, UMR CNRS 7193, ISTEP, 75005 Paris, France

Stanimir A. Bonev
Lawrence Livermore National Laboratory, Livermore, California 94550, USA and Department of Physics, Dalhousie University, Halifax, Nova Scotia B3H 3J5, Canada

Majdi Hochlaf
Université Paris-Est, Laboratoire Modélisation et Simulation MultiEchelle, MSME UMR 8208 CNRS, 77454 Marne-La-Vallée, France

Helen E. Maynard-Casely†
School of Chemistry, University of Edinburgh, United Kingdom
(Received 23 December 2012; published 24 June 2013)

We report results from high pressure and temperature experiments that provide evidence for the reactivity of xenon with water ice at pressures above 50 GPa and a temperature of 1500 K—conditions that are found in the interiors of Uranus and Neptune. The x-ray data are sufficient to determine a hexagonal lattice with four Xe atoms per unit cell and several possible distributions of O atoms. The measurements are supplemented with *ab initio* calculations, on the basis of which a crystallographic structure with a $Xe_4O_{12}H_{12}$ primitive cell is proposed. The newly discovered compound is formed in the stability fields of superionic ice and η-O_2, and has the same oxygen subnetwork as the latter. Furthermore, it has a weakly metallic character and likely undergoes sublattice melting of the H subsystem. Our findings indicate that Xe is expected to be depleted in the atmospheres of the giant planets as a result of sequestration at depth.

DOI: 10.1103/PhysRevLett.110.265501 PACS numbers: 62.50.−p, 61.05.cp, 96.15.Bc, 96.30.Pj

Knowledge of the chemistry of xenon (Xe) with planetary materials under high pressure P and temperature T conditions is a prerequisite for understanding the abundance of Xe and its isotopic ratios in the atmospheres of giant planets. The noble gases Ne, Ar, Kr, and Xe are indeed among the most critical heavy elements [1], as their abundances constrain the models for giant planet formation and the origin of their atmospheres. The field of Xe chemistry at ambient P was initiated with the synthesis of fluoride salts [2] and later extended to H, C, O, N, S, other halogens, and even metals (Au, Hg), so that close to a hundred Xe compounds are currently known [3,4]. However, the use of pressure as a means to enforce Xe to bond to other elements has seldom been investigated [5]. Geophysicists first started to explore this track as a potential explanation for the observed Xe deficiency in the terrestrial and Martian atmospheres [6]. Xe-Fe compounds were shown to be unstable up to 70 GPa [7], although up to 0.8 mol% Xe could be alloyed to Fe at 300 GPa [8]. It was later proposed that Xe depletion from Earth's atmosphere could occur by Xe substitution for Si in the silicates network under the P-T conditions of the deep crust and mantle, therefore forming Xe-doped oxides [9–11], a synthesis shortly followed by that of pure XeO_2 at ambient P [12].

Water ice is one of the most prevalent substances in the Solar System, with the majority of it existing at high P and T conditions in the interiors of giant planets. Xe is among the gases that stabilizes clathrate hydrate structures through van der Waals interactions. However, Xe hydrates are stable only up to 2.5 GPa, before dissociating into Xe plus ice VII [13]. The chemistry of Xe with water has nonetheless been successfully explored by UV photolysis of water in solid Xe at ambient pressure. Among the compounds hitherto obtained are HXeOH [14] and, the latest one to date, HXeOXeH [15], which results from the insertion of Xe atoms in the water molecule. These results reopened the perspective to synthesize covalent compounds in the Xe-H_2O system by applying extreme P-T conditions.

In this Letter we report the first experimental evidence for the reactivity of Xe with water ice at conditions found in the interior of giant planets. The resulting crystalline structure is resolved from x-ray diffraction data with additional input from *ab initio* calculations. Our analysis indicates the participation of H in the structure formation, and brackets for the H content are given with an emphasis on the $Xe_4O_{12}H_{12}$ structure.

High P-high T conditions were produced in laser-heated diamond-anvil cells and x-ray diffraction experiments were carried out *in situ* on the ID27 beam line of the

ESRF. A ring was laser cut in a 2.5 μm thick platinum (Pt) foil and inserted in a 80 μm hole drilled in a rhenium gasket on top of two ruby spheres, with Pt acting as a coupler with the IR laser. Milli-Q deionised water was then loaded in the sample chamber, and Xe was added cryogenically in a N_2 atmosphere. The sample did not contain N_2 after closing the cell as attested by the absence of the N_2 vibron in Raman spectra. The pressure was measured from the ruby fluorescence signal [16], and the temperature was calculated from the thermal equation of state of Pt [17]. Temperatures were also measured from the sample thermal emission spectra. However, volumes measured from the x-ray diffraction patterns show that the sample T was lower than the surface T as previously shown when a metallic laser coupler is used [18]. Data were collected on a MAR-CCD using a monochromatic x-ray beam ($\lambda = 0.3738$ Å) focused to a 3×4 μm area on the sample. We carried out experiments at P ranging from 17 to 80 GPa and T below the melting point of water ice.

During laser heating at 50 GPa, we observed two phases above 1500 K in addition to Xe, Pt, and bcc ice and will refer to them as phase-1 and phase-2 (see Fig. 1). X-ray diffraction peaks from phase-1 can be assigned to a face-centered cubic structure. Phase-1 is not quenchable back to room T and is equally observed in blank experiments on Pt-water mixtures. No blank experiment was conducted on the Xe-Pt system as it has been experimentally explored at P-T conditions covering those of the present work and no reaction was observed [7]. Phase-2 is stable back to room T and was systematically synthesized upon heating up to 80 GPa, the maximum P investigated here. The x-ray diffraction signal from phase-2 is indexed by a hexagonal cell with $a = b = 5.0539 \pm 0.0003$ Å and $c = 8.210 \pm 0.001$ Å at 58 GPa and 1500 K. Its compressibility as obtained from a second-order Birch-Murnaghan equation of state is 77 ± 5 GPa at room T (fitted with zero pressure volume parameter $V_0 = 255.8$ Å^3), and 67 ± 5 GPa at 1500 K ($V_0 = 269.8$ Å^3). The thermal expansion coefficient at high P is $(1.8 \pm 0.1) \times 10^{-5}$ K^{-1} (see Fig. 2).

The x-ray diffraction pattern at 58 GPa and 1500 K has a sufficiently high powder-quality pattern for the atomic positions of the Xe and oxygen (O) to be refined; $P63/mmc$ is the highest-symmetry space group allowed. From density considerations, four atoms of Xe can be accommodated in the unit cell. The solution is however not unique for the O atoms, with three possibilities equally well satisfying the x-ray pattern intensities. The three possible structures are with either 12, 14, or 16 O atoms per unit cell. In order to determine the correct solution for O atoms and to investigate the presence of hydrogen in the structure, we have carried out a theoretical analysis.

First principles density functional theory calculations were carried out with VASP [19] using projector augmented wave pseudopotentials with 8 and 6 valence electrons for the Xe and O atoms, respectively, and a 500 eV plane wave cutoff. Full structural optimizations were performed with a uniform $6 \times 6 \times 6$ $\mathbf{k}$-point grid sampling of the Brillouin zone, which ensures the desired degree of convergence (meV/atom). The choice of exchange-correlation functional can lead to significant variations in the specific volume of the Xe-O-H systems being studied. In order to provide an estimate for the theoretical uncertainties originating from the exchange-correlation approximation, we have carried out calculations within the local density approximation, the Perdew-Burke-Ernzerhof [20]

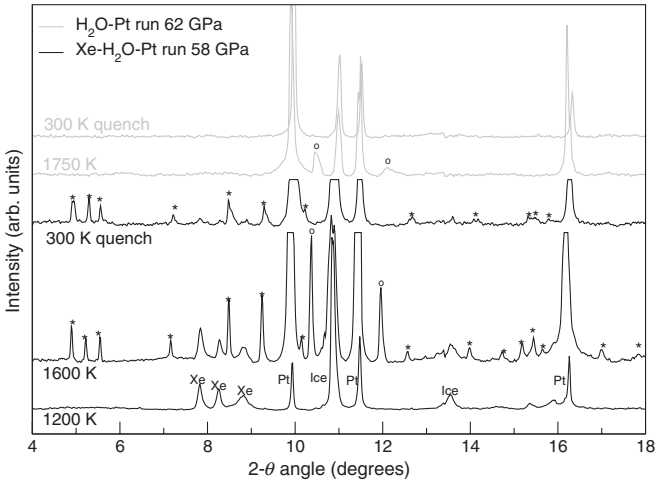

FIG. 1. X-ray diffraction patterns. Spectra obtained upon and after heating a Xe + H_2O + Pt sample (black lines) and upon and after heating a H_2O + Pt sample (gray lines). Circles indicate peaks from phase-1 and asterisks indicate peaks from phase-2.

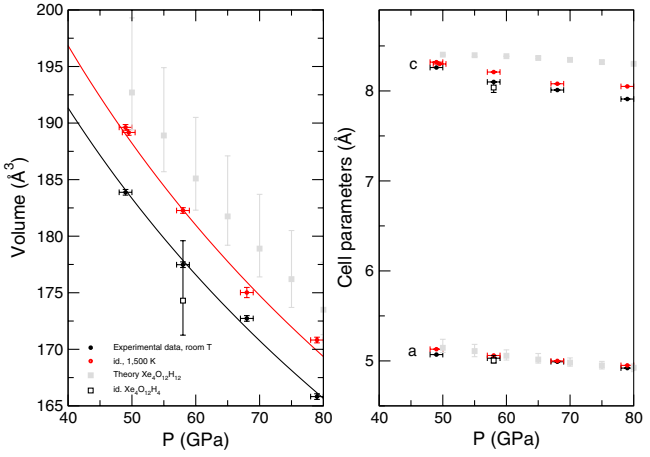

FIG. 2 (color online). Pressure dependence of the unit cell volume (left) and cell parameters (right). Solid curves are a second-order Birch-Murnaghan fit to the data. Theoretical calculations: squares are results obtained with the PBEsol functional, the error bars extend from results obtained using the local density approximation (lower bar) to results within the PBE (upper bar).

generalized gradient approximation (PBE), and the PBE revised for solids [21] (PBEsol). Additionally, for selected structures van der Waals interactions were included using the vdW-D2 method [22] as implemented in VASP. However, this did not change the results.

Given the fact that the newly synthesized structure is thermodynamically stable only at high T, as well as its complexity, we have not attempted to perform a complete phase space crystalline search. Instead, we have limited the theoretical analysis to within the constraints imposed by the experimental data. Starting from the experimental lattice parameters and refined atomic positions, structural relaxations were initially performed on systems with Xe and O atoms only. The optimizations with 16, 14, and 12 O atoms resulted in theoretically stable structures that differ significantly from the experimental fits—respectively $+1\%$, -7%, and -5% in the a lattice parameter, and $+6\%$, $+8\%$, and $+9\%$ in the c lattice parameter (within the PBE). The internal O coordinates also change significantly. These structural differences, which are accompanied by large energy differences on the order of tens of eV/atom, are beyond the uncertainties of both the theoretical and experimental methods. The fact that no H-free structure could be identified is in agreement with a recent theoretical investigation [23] where no thermodynamically stable xenon oxides were found below 83 GPa.

Analysis for the effect of hydrogen was carried out by initially placing H atoms into the system both at random positions and at selected high-symmetry points. This was followed by full structural optimization at 58 GPa. To ensure that the entire phase space for H positions had been sampled, we also performed selective molecular dynamics where the H subsystem was heated while Xe and O atoms were held fixed. This procedure was repeated with 4, 12, and 24 H atoms. For the structures with 16 and 14 O atoms per unit cell, adding H atoms increases even further the discrepancy with the experimental fits. Therefore, the structures with 16 and 14 O atoms can be ruled out conclusively. On the other hand, introducing H in calculations with 12 O atoms per unit cell yields structures that match the x-ray data. The best fitting result is for 12 H atoms, for which the finite temperature lattice parameters, optimized to give an isotropic stress tensor at each P–300 K point, are compared with the measured ones (see Fig. 2). Using 4 H atoms, the calculated structure has an excellent agreement with the measured volume (see Fig. 2); however, the H coordinates cannot be reproduced within any hexagonal space group. The structures with 24 H atoms do not give satisfactory agreement with the experimental cell parameters. It is nonetheless difficult to determine theoretically the exact H content—between 4 and 12 atoms per unit cell. In fact, it may be varied due the diffusive character of H at high temperature as described below. To answer these questions requires a full free energy thermodynamic stability analysis at 1500 K, which goes beyond the scope of this Letter.

The optimized Xe and O atomic positions further refined for the $Xe_4O_{12}H_{12}$ structure by a Rietveld fit to the data (see Fig. 3) are a 12(k) site (x, y, z) for O with $x = 0.157 \pm 0.002$, $y = 0.314 \pm 0.003$, $z = 0.622 \pm 0.002$, and a 4(f) site (1/3, 2/3, z) for Xe with $z = 0.071 \pm 0.001$. The H atoms, according to the theoretical calculations, are located on a 12(j) site (x, y, 1/4) with $x = 0.9427 \pm 0.002$, $y = 0.2886 \pm 0.004$. The structure consists of two $Xe_2O_6H_6$ units per unit cell (see the inset of Fig. 3), and the Xe-O distance is 2.21 ± 0.01 Å. This distance is similar to that observed in the HXeOH and HXeOXeH molecules, and equal to 2.208 Å and 2.15 Å, respectively [14,15].

In order to examine the finite temperature properties of the $Xe_4O_{12}H_{12}$ structure, we performed density functional theory molecular dynamics simulations on supercells containing 224 and 504 atoms and Γ-point sampling of the Brillouin zone. While the simulations with the two cell sizes give very close results, we determined that a denser **k**-point grid is required for well converged results. Nevertheless, it is worth noting the observed tendency of the H subsystem to become diffusive at finite T. Its self-diffusion coefficient is estimated to be 5 $Å^2\,ps^{-1}$ at 60 GPa and 1500 K. The diffusivity of H is similar to what is observed in H_2O at these conditions, except that while water is superionic $Xe_4O_{12}H_{12}$ is metallic. The electronic properties of the latter, computed within the PBEsol, are shown in Fig. 4. Notice that the electronic states near the Fermi level are due to the Xe and O atoms, so that the metallic character would be preserved even if H undergoes subatomic melting at high T.

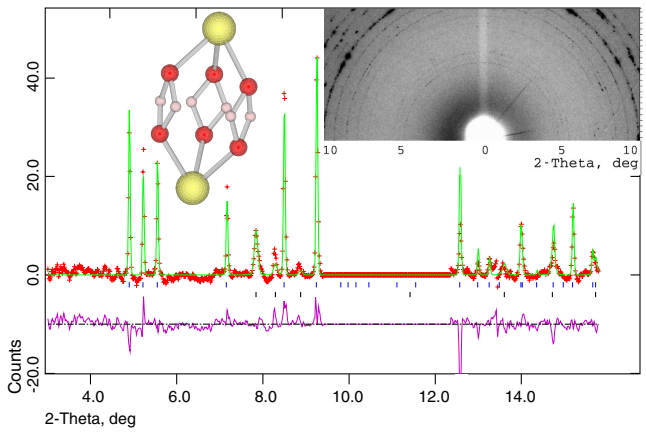

FIG. 3 (color online). Rietveld fit of the $Xe_4O_{12}H_{12}$ structure at 58 GPa and 1500 K. Vertical ticks indicate diffraction peaks from phase-2 (blue) and from Xe (black). The pattern has been cut between 9.4 and 12.3 degrees, as the signal in this region is overloaded by Pt and water ice diffraction peaks which would prevent an accurate refinement of the less intense $Xe_4O_{12}H_{12}$ peaks. Insets: structure of the $Xe_2O_6H_6$ unit (two per cell), and inner half of the corresponding 2D diffraction pattern. [The ring at 10 degrees is the (111) Pt peak; all rings inwards are from either phase-2 or Xe].

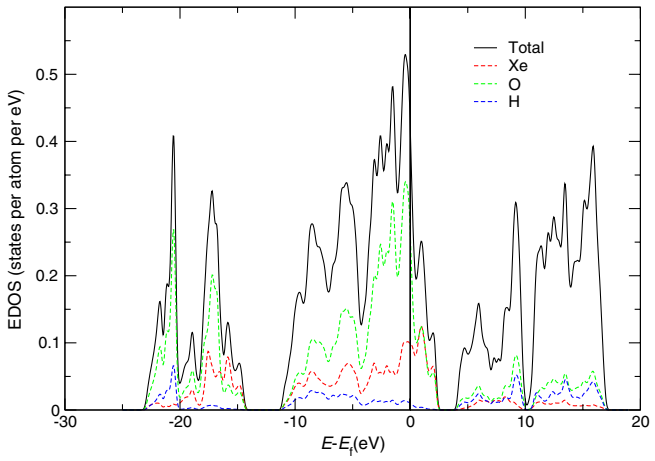

FIG. 4 (color online). Electronic density of states (EDOS) of $Xe_4O_{12}H_{12}$ computed at 60 GPa within the PBEsol. The total EDOS are shown with a solid line. The dashed lines indicate partial EDOS projected on different atomic species (as indicated in the figure legend). The energy scale is shifted so that the Fermi level is at 0.

No oxygen phase was detected in the x-ray diffraction patterns. However, the $Xe_4O_{12}H_{12}$ structure we propose may remarkably be obtained by the interpenetration of the high-P Xe and η-O_2 hcp structures [24]. The O atoms in the unit cell of the newly discovered phase can be matched by summing four η-O_2 unit cells expanded by 25% along the c axis, i.e., along the intramolecular bond, resulting within 1% in an identical atomic volume for O between both phases. η-O_2 has been described to be stable below the O_2 melting line between 15 and 20 GPa [25], but recent experiments carried out at much higher P evidenced another domain of stability just below the melting line above 44 GPa [26]. The stability field of the new Xe compound as mapped in this study thus coincides with that of high P η-O_2. In contrast to other O_2 solid phases, η-O_2 is characterized by its orientational disorder and a high degree of charge transfers that provides an explanation for the relatively short Xe-O distance in our present phase. It is also interesting to note that the $Xe_4O_{12}H_{12}$ structure bears similarities to the hypothetical clathrate V structure proposed [27] for $4X$-$8Y$-$68H_2O$, where $X = CCl_4$ and $Y =$ Xe, with partial occupancy for the latter. Both are hexagonal with the $P63/mmc$ space group, an $\ldots ABAB\ldots$ stacking sequence, and a c/a ratio of 1.61.

Although theoretical calculations reproduced the experimental results without considering Pt, its role in the energetics of the reaction has to be considered as its hydrogenation is an exothermic reaction [28]. A PtH x-ray diffraction signal [29] was observed locally upon heating at 40 GPa, a P value lower than that of Xe reactivity. It is therefore not possible to decipher between newly formed and inherited PtH from previous heating cycles at lower P. PtH was never observed simultaneously with the Xe compound (see Fig. 1), but that could be due to the very small x-ray beam (3×4 μm) and high diffusion rate of hydrogen. In addition, Raman spectra collected after heating showed no sign of a H_2 vibron. We therefore propose the following global reaction:

$$2\mathrm{Xe} + 6\mathrm{H_2O} + (12 - x/2)\mathrm{Pt} \rightarrow \mathrm{Xe_2O_6H}_{x/2} + (12 - x/2)\mathrm{PtH}. \quad (1)$$

The reaction must have a negative $\Delta V/V$ value to be pressure induced, which further brackets the H content between 8 ($\Delta V/V = -0.2\%$ per mole) and 12 ($\Delta V/V = -2.2\%$ per mole) atoms per cell.

Water ice and Xe are consequently expected to react at P-T conditions higher than 50 GPa and 1500 K. These conditions are gathered inside giant planets, and particularly within Uranus and Neptune that contain a larger proportion of planetary ices. These conditions are also gathered within subducted slabs in the deep Earth, provided that sea-water carries Xe within the deep mantle [30]. The observed enrichment of the Jovian atmosphere in noble gases by a factor of 2 compared to the solar abundances has been explained by different scenarios including their clathration and/or absorption on water ice in preplanetary objects and their further release into the planet's atmosphere [31]. However, Xe abundance is overestimated in these scenarios. Any reactivity with Xe at depth would explain this mismatch and future probe missions to Saturn [32], Uranus, and Neptune could provide a test of the present results. These planetary implications also fit into the wider context of noble gases sequestration at depth inside giant planets as demonstrated for Ne in the interiors of Jupiter [33].

We acknowledge the ESRF for provision of beam time on ID27 and LLNL for computational resources. We thank M. Mezouar and E. Gregoryanz for their help with collecting *in situ* x-ray diffraction data, and Y. Noel and M. Marques for useful discussions. C. S. is funded by the European Research Council under the European Community's Seventh Framework Programme (Grants No. FP7/2007-2013 and No. 259649). S. A. B. performed work at LLNL under the auspices of the U.S. Department of Energy under Grant No. DE-AC52-07NA27344.

*Present address: School of Physics and Astronomy and Center for Science at Extreme Conditions, University of Edinburgh, Edinburgh EH9 3JZ, United Kingdom.
†Present address: Bragg Institute, Australian Nuclear Science and Technology Organisation, Menai, New South Wales 2234, Australia.

[1] T. Guillot, Annu. Rev. Earth Planet Sci. **33**, 493 (2005).
[2] N. Bartlett, Proc. Chem. Soc. 218 (1962).
[3] W. Grochala, Chem. Soc. Rev. **36**, 1632 (2007).
[4] R. B. Gerber, Annu. Rev. Phys. Chem. **55**, 55 (2004).

[5] M. Somayazulu, P. Dera, A. F. Goncharov, S. A. Gramsch, P. Liermann, W. Yang, Z. Liu, H. k. Mao, and R. J. Hemley, Nat. Chem. **2**, 50 (2009).
[6] E. Anders and T. Owen, Science **198**, 453 (1977).
[7] W. A. Caldwell, J. H. Nguyen, B. G. Pfrommer, F. Mauri, S. G. Louie, and R. Jeanloz, Science **277**, 930 (1997).
[8] K. M. Lee and G. Steinle-Neumann, J. Geophys. Res. **111**, B02202 (2006).
[9] C. Sanloup, B. C. Schmidt, E. C. Perez, A. Jambon, E. Gregoryanz, and M. Mezouar, Science **310**, 1174 (2005).
[10] M. I. J. Probert, J. Phys. Condens. Matter **22**, 025501 (2010).
[11] C. Sanloup, B. C. Schmidt, G. Gudfinnsson, A. Dewaele, and M. Mezouar, Geochim. Cosmochim. Acta **75**, 6271 (2011).
[12] D. S. Brock and G. J. Schrobilgen, J. Am. Chem. Soc. **133**, 6265 (2011).
[13] C. Sanloup, H.-K. Mao, and R. J. Hemley, Proc. Natl. Acad. Sci. U.S.A. **99**, 25 (2002).
[14] M. Pettersson, J. Lundell, and M. Räsänen, Eur. J. Inorg. Chem. **1999**, 729 (1999).
[15] L. Khriachtchev, K. Isokoski, A. Cohen, M. Räsänen, and R. B. Gerber, J. Am. Chem. Soc. **130**, 6114 (2008).
[16] H. K. Mao, J. Xu, and P. M. Bell, J. Geophys. Res. **91**, 4673 (1986).
[17] C.-S. Zha, K. Mibe, W. A. Bassett, O. Tschauner, H.-K. Mao, and R. J. Hemley, J. Appl. Phys. **103**, 054908 (2008).
[18] J. F. Lin, M. Santoro, V. V. Struzhkin, H. K. Mao, and R. J. Hemley, Rev. Sci. Instrum. **75**, 3302 (2004).
[19] G. Kresse and J. Hafner, Phys. Rev. B **47**, 558 (1993); G. Kresse and X. Furthmuller, Comput. Mater. Sci. **6**, 15 (1996).
[20] J. P. Perdew, K. Burke, and M. Ernzerhof, Phys. Rev. Lett. **77**, 3865 (1996).
[21] J. P. Perdew, A. Ruzsinszky, G. I. Csonka, O. A. Vydrov, G. E. Scuseria, L. A. Constantin, X. Zhou, and K. Burke, Phys. Rev. Lett. **100**, 136406 (2008).
[22] S. Grimme, J. Comput. Chem. **27**, 1787 (2006).
[23] Q. Zhu, D. Y. Jung, A. R. Oganov, C. W. Glass, C. Gatti, and A. O. Lyakhov, Nat. Chem. **5**, 61 (2013).
[24] L. F. Lundegaard, C. Guillaume, M. I. McMahon, E. Gregoryanz, and M. Merlini, J. Chem. Phys. **130**, 164516 (2009).
[25] M. Santoro, E. Gregoryanz, H.-K. Mao, and R. J. Hemley, Phys. Rev. Lett. **93**, 265701 (2004).
[26] A. F. Goncharov, T. R. R. N. Subramanian, M. Somayazulu, V. B. Prakapenka, and R. J. Hemley, J. Chem. Phys. **135**, 084512 (2011).
[27] E. A. Smelik and H. E. King, Z. Kristallogr. **211**, 84 (1996).
[28] L. Visscher, T. Saue, W. C. Nieuwpoort, K. Faegri, and O. Gropen, J. Chem. Phys. **99**, 6704 (1993).
[29] T. Scheler, O. Degtyareva, M. Marques, C. L. Guillaume, J. E. Proctor, S. Evans, and E. Gregoryanz, Phys. Rev. B **83**, 214106 (2011).
[30] G. Holland and C. J. Ballentine, Nature (London) **441**, 186 (2006).
[31] F. Hersant, D. Gautier, and J. I. Lunine, Planet. Space Sci. **52**, 623 (2004).
[32] B. Marty, T. Guillot, A. Coustenis, N. Achilleos, Y. Alibert, S. Asmar, D. Atkinson, S. Atreya, G. Babasides, K. Baines, T. Balint, D. Banfield, S. Barber, B. Bezard, G. L. Bjoraker, M. Blanc, S. Bolton, N. Chanover, S. Charnoz, E. Chassefiere, J. E. Colwell, E. Deangelis, M. Dougherty, P. Drossart, F. M. Flasar, T. Fouchet, R. Frampton, I. Franchi, D. Gautier, L. Gurvits, R. Hueso, B. Kazeminejad, T. Krimigis, A. Jambon, G. Jones, Y. Langevin, M. Leese, E. Lellouch, J. Lunine, A. Milillo, P. Mahaffy, B. Mauk, A. Morse, M. Moreira, X. Moussas, C. Murray, I. Mueller-Wodarg, T. C. Owen, S. Pogrebenko, R. Prange, P. Read, A. Sanchez-Lavega, P. Sarda, D. Stam, G. Tinetti, P. Zarka, J. Zarnecki, and Kronos Consortium, Exp. Astron. **23**, 947 (2009).
[33] H. F. Wilson and B. Militzer, Phys. Rev. Lett. **104**, 121101 (2010).